

## Supplementary information

### **Flexible and fire-retardant silica/cellulose aerogel using bacterial cellulose nanofibrils as template material**

Björn K. Birdsong<sup>a\*</sup>, Qiong Wu<sup>a</sup>, Mikael S. Hedenqvist<sup>a</sup>, Antonio J. Capezza<sup>a</sup>, Richard L. Andersson<sup>a</sup>, Anna J. Svagan<sup>a</sup>, Oisik Das<sup>b</sup>, Rhoda Afriyie Mensah<sup>b</sup>, Richard T. Olsson<sup>a\*</sup>.

<sup>a</sup>Department of Fibre and Polymer Technology, KTH Royal Institute of Technology, Teknikringen 58, 11428, Stockholm, Sweden.

<sup>b</sup>Department of Civil, Environmental and Natural Resources Engineering, Luleå University of Technology, 97187 Lulea, Sweden

Corresponding authors.

*E-mail address:* \*[birdsong@kth.se](mailto:birdsong@kth.se) (B. K. Birdsong)

*E-mail address:* \*[rols@kth.se](mailto:rols@kth.se) (R. T. Olsson)

**Table. S1.** The average thicknesses of the obtained fibers and secondary SiO<sub>x</sub> particles (spherical particles) were estimated with ImageJ® using 50 randomly selected fibers and particle measurements using field emission scanning electron microscope (FE-SEM) images. The coating thicknesses was calculated by subtracting the virgin bCNF from the measured fiber thickness and dividing by two. The values should be regarded as approximations due to the differences in morphology.

Thickness			
	Fiber (nm)	Coating (nm)	Secondary SiO <sub>x</sub> particle diameter (nm)
bCNF	15.4±3.6	-	-
APTES-bCNF (Low)	58.6±18.9	~22	-
APTES-bCNF (Medium)	46.0±15.5	~16	-
APTES-bCNF (High)	50.8±21.7	~18	-
MTMS-bCNF (Low)	30.7±13.2	~8	-
MTMS-bCNF (Medium)	20.4±5.2	~3	-
MTMS-bCNF (High)	38.2±10.8	~12	85.6487±28.6
TEOS-bCNF (Low)	29.3±7.7	~7	34.51336±14.7
TEOS-bCNF (Medium)	31.0±10.0	~8	39.77434±10.4
TEOS-bCNF (High)	20.6±5.6	~3	85.6408±22.8

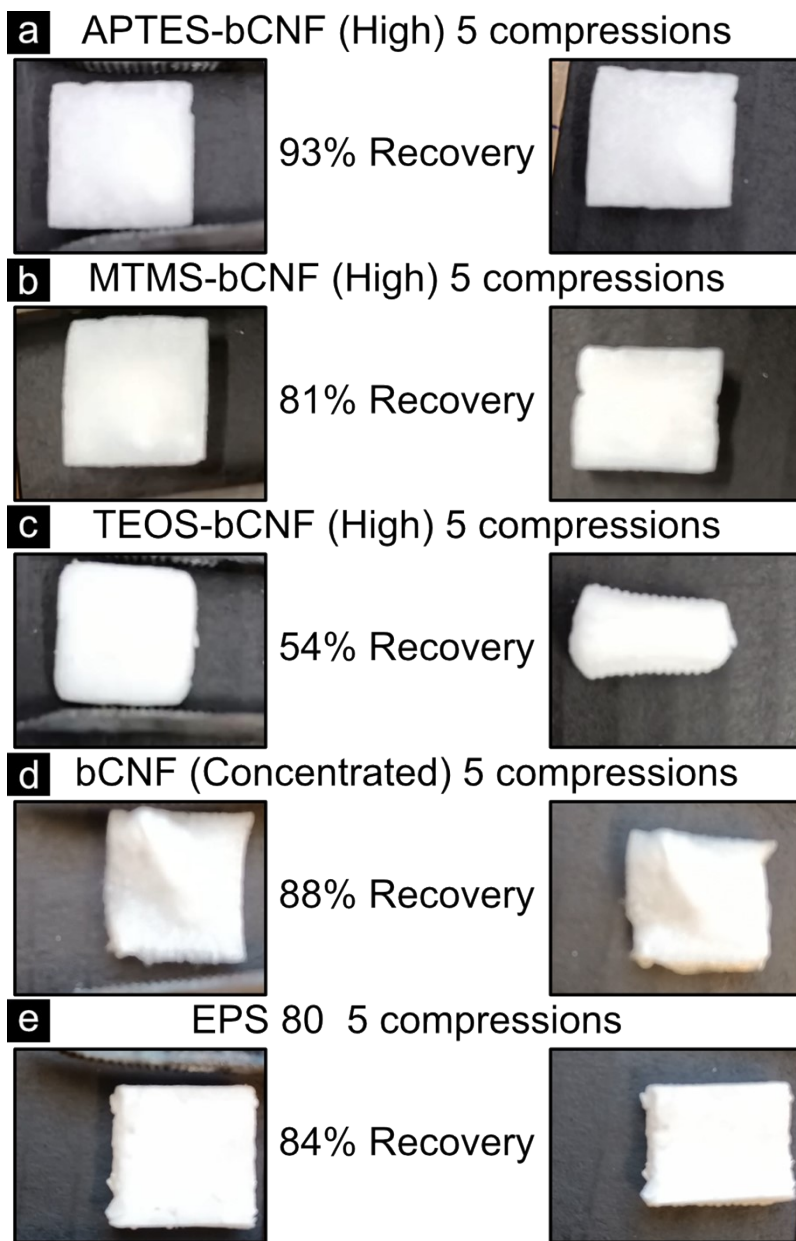


**Fig. S1** Depicts the aerogels after 5 compression cycles to *ca.* 50 % of the original width. Recovery was measured using the final width of the material compared to the original width.

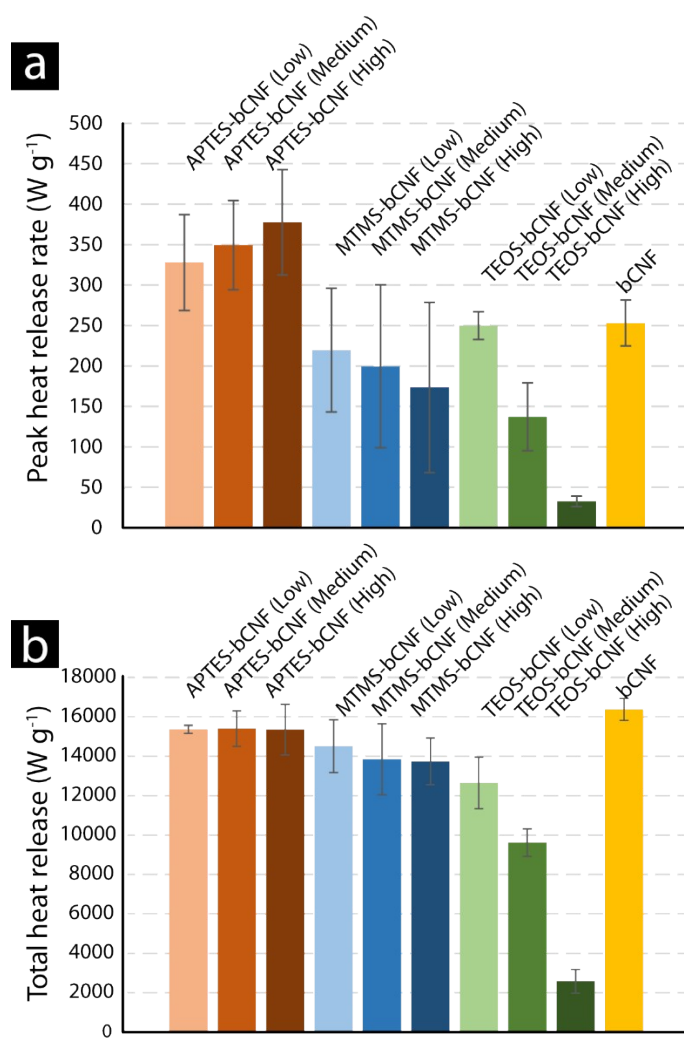


**Fig. S2** Depicts the Peak heat release rate (PHRR) (a) and total heat release (THR) (b), for all obtained foam materials obtained using Micro-scale calorimetry (MCC). Although the PHRR of TEOS-bCNF (Low) was higher compared to MTMS-bCNF (Low), the THR for TEOS-bCNF (Low) was lower, indicating that the combustion of material occurred more instantaneously in the case of TEOS-bCNF (Low) while a more spread out combustion occurred for MTMS-bCNF (Low) as seen in Fig. S3g.

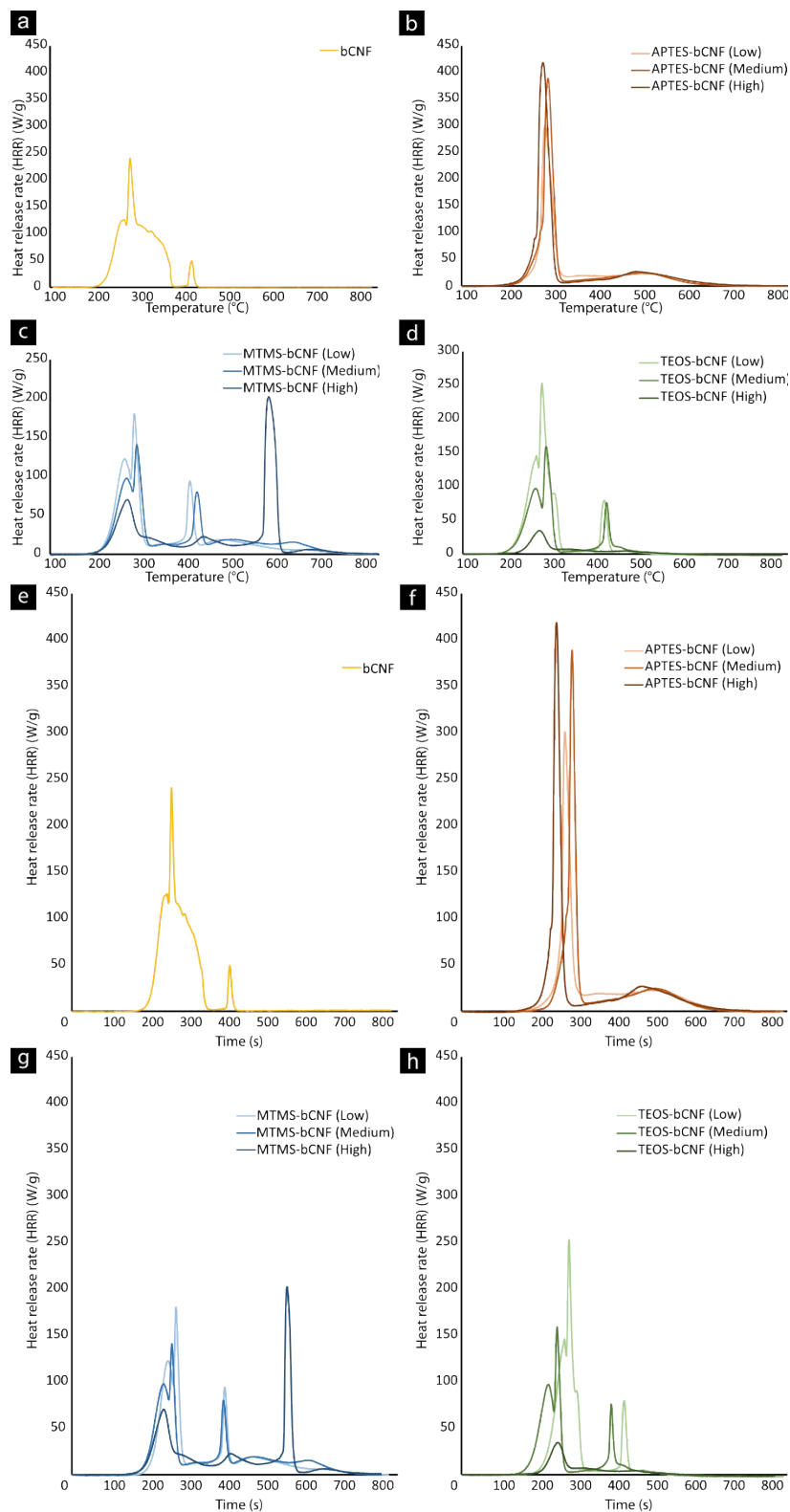


**Fig. S3** Shows representative curves for heat release rate vs. temperature (a-d) and heat release rate vs. time (e-h) for all obtained foam materials obtained using microscale combustion calorimetry (MCC), allowing for comparison of potential fire properties of materials.

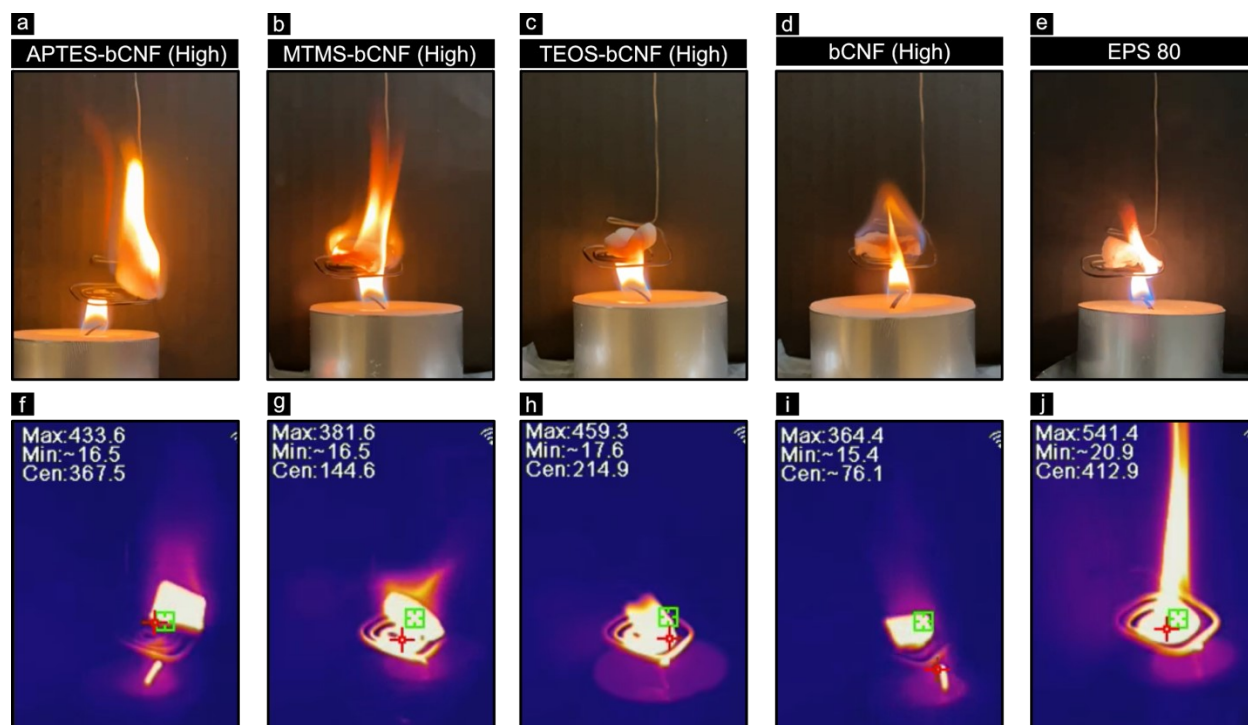


**Fig. S4** photographs of aerogel materials mounted on steel wire and ignited using a candle flame (a-e) and the corresponding infrared images of the same aerogel materials during combustion (f-j). Entire videos are found as additional attachments.

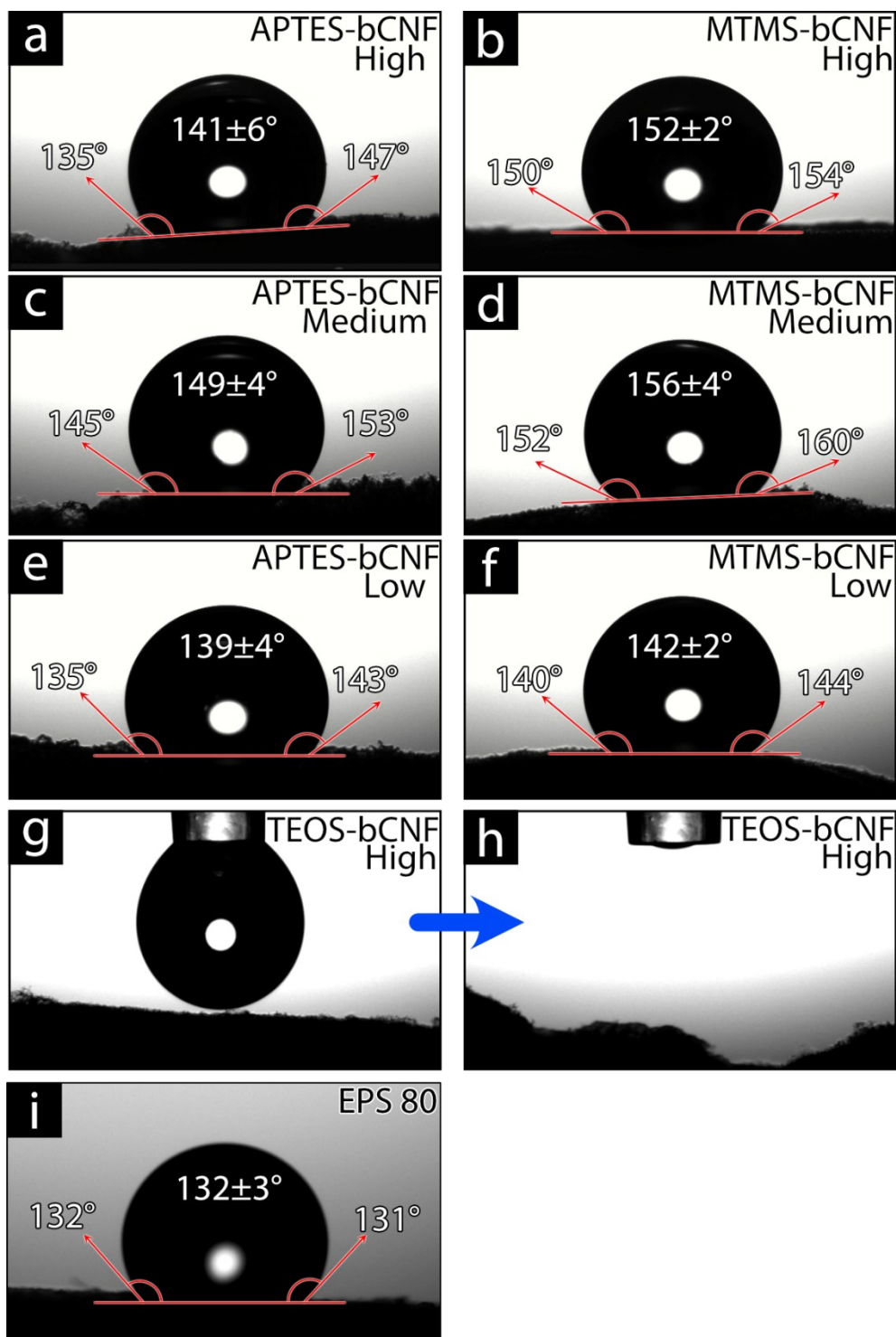


**Fig. S5.** Depicts the contact angle obtained on virgin non-pressed aerogel materials (a-h) and EPS 80 foam (i).

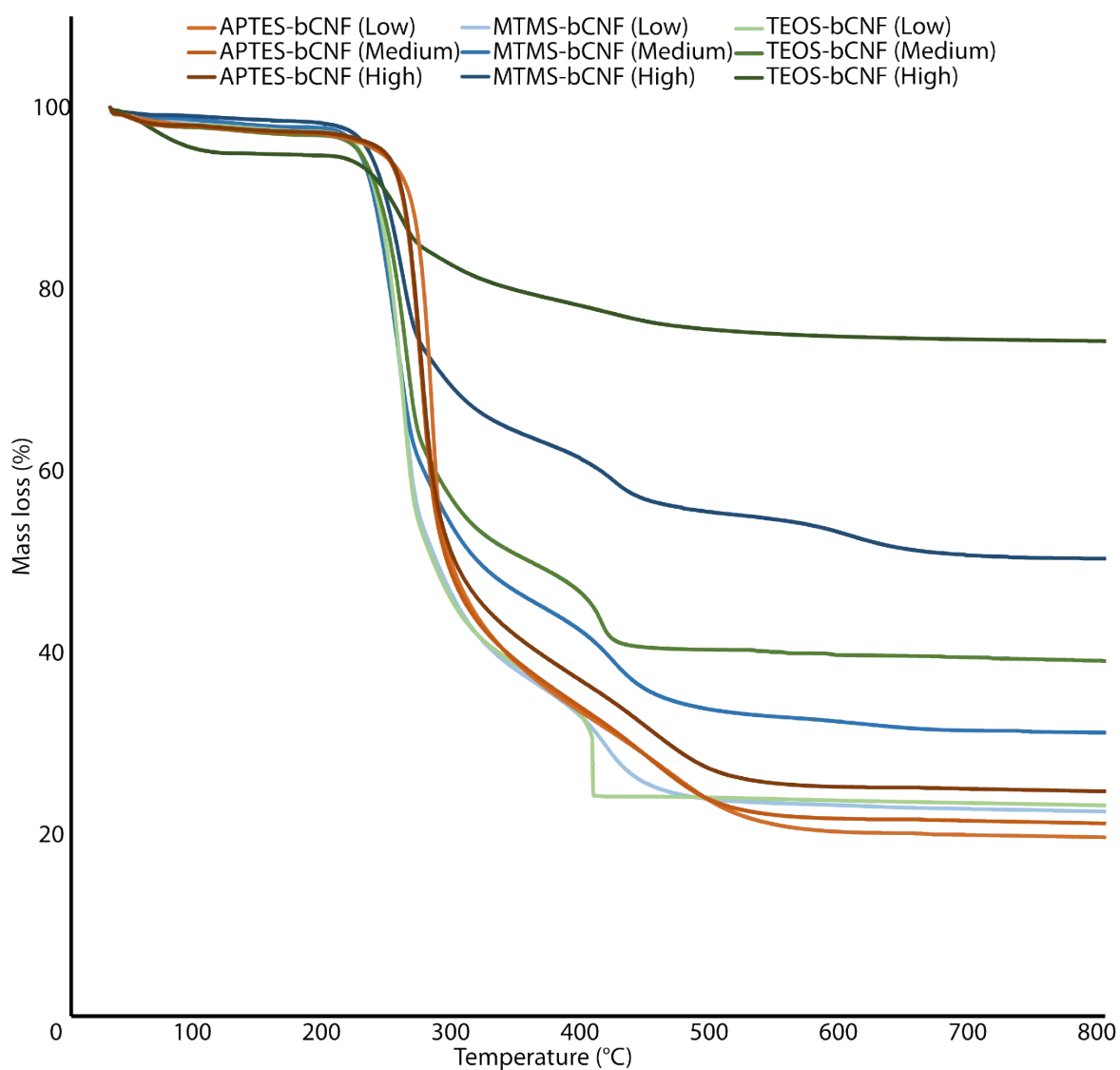


**Fig. S6.** Depicts the obtained curves from the thermogravimetric analysis (TGA) for all foam materials. Where APTES-coated bCNF (Low, Medium, and High) is depicted in orange, MTMS-bCNF (Low, Medium, and High) in blue, and TEOS-bCNF (Low, Medium, and High) in green. The sharp drop in mass seen for TEOS-bCNF (Low) at *ca.* 400 °C was attributed to the more rapid degradation of the material's bCNF component, which was further confirmed from MCC (Fig. S3h).